SCIENTIFIC REP♦RTS

OPEN

Incomplete Ionization of a 110 meV Unintentional Donor in β-Ga$_2$O$_3$ and its Effect on Power Devices

Adam T. Neal[1,2], Shin Mou[1], Roberto Lopez[3], Jian V. Li[3], Darren B. Thomson[4], Kelson D. Chabak[4] & Gregg H. Jessen[4]

Understanding the origin of unintentional doping in Ga$_2$O$_3$ is key to increasing breakdown voltages of Ga$_2$O$_3$ based power devices. Therefore, transport and capacitance spectroscopy studies have been performed to better understand the origin of unintentional doping in Ga$_2$O$_3$. Previously unobserved unintentional donors in commercially available ($\bar{2}$01) Ga$_2$O$_3$ substrates have been electrically characterized via temperature dependent Hall effect measurements up to 1000 K and found to have a donor energy of 110 meV. The existence of the unintentional donor is confirmed by temperature dependent admittance spectroscopy, with an activation energy of 131 meV determined via that technique, in agreement with Hall effect measurements. With the concentration of this donor determined to be in the mid to high 10^{16} cm^{-3} range, elimination of this donor from the drift layer of Ga$_2$O$_3$ power electronics devices will be key to pushing the limits of device performance. Indeed, analytical assessment of the specific on-resistance (R$_{onsp}$) and breakdown voltage of Schottky diodes containing the 110 meV donor indicates that incomplete ionization increases R$_{onsp}$ and decreases breakdown voltage as compared to Ga$_2$O$_3$ Schottky diodes containing only the shallow donor. The reduced performance due to incomplete ionization occurs in addition to the usual tradeoff between R$_{onsp}$ and breakdown voltage.

While crystalline Ga$_2$O$_3$ has been known for many years, the recent availability of high quality crystalline substrates[1] and the demonstration of Ga$_2$O$_3$ MESFETs[2] and MOSFETs[3–6] have motivated interest in Ga$_2$O$_3$ for next generation ultra-wide bandgap power electronics applications. With a bandgap of 4.5–4.9 eV and estimated critical breakdown field of 8 MV/cm, Ga$_2$O$_3$ possesses a Baliga figure of merit 10 times greater than SiC and four times greater than GaN[2]. Indeed, even at this early stage of development, electric fields of at least 3.8 MV/cm[4] and 5.1 MV/cm[7] have been demonstrated in lateral Ga$_2$O$_3$ FETs and vertical Schottky diodes, respectively, already surpassing bulk critical fields of GaN and SiC. In addition to these promising material properties, melt-growth methods for bulk Ga$_2$O$_3$ substrate growth[8–17] are expected to be more cost-effective than the sublimation techniques used for the growth of SiC substrates, lowering manufacturing costs for Ga$_2$O$_3$ based power electronics.

While the large breakdown electric field demonstrated in these early experimental studies is certainly promising, pushing the breakdown voltages of Ga$_2$O$_3$ based power electronics devices towards their predicted limits requires further work to understand and eliminate unintentional doping in the material. To illustrate this fact, the dependence of breakdown voltage of p-n single-sided junction and Schottky junction devices, normalized by material parameters, is plotted in Fig. 1. The black line indicates the theoretical limit, assuming the full-depletion approximation and one dimensional electrostatics. By normalizing the breakdown voltages in this way, one can isolate the effect of doping on device breakdown voltage to allow comparisons of devices made from different materials. Comparing early Ga$_2$O$_3$ devices to those of more mature semiconductor materials gives insight into the future potential of Ga$_2$O$_3$ devices. The plotted experimental data are among the best reported for vertical devices of each material with large breakdown voltage and low doping of the device drift-layer. While edge effects prevent real devices of any material from matching the simplified theoretical limit exactly, the N_d^{-1} trend is nevertheless observed considering the best performing devices of the different material systems. Comparing Ga$_2$O$_3$ to the

[1]Air Force Research Laboratory, Materials and Manufacturing Directorate, Wright Patterson AFB, OH, USA. [2]Universal Technology Corporation, Dayton, OH, USA. [3]Texas State University, Department of Physics, San Marco, TX, USA. [4]Air Force Research Laboratory, Sensors Directorate, Wright Patterson AFB, OH, USA. Correspondence and requests for materials should be addressed to A.T.N. (email: adam.neal.2.ctr@us.af.mil) or S.M. (email: shin.mou.1@us.af.mil)
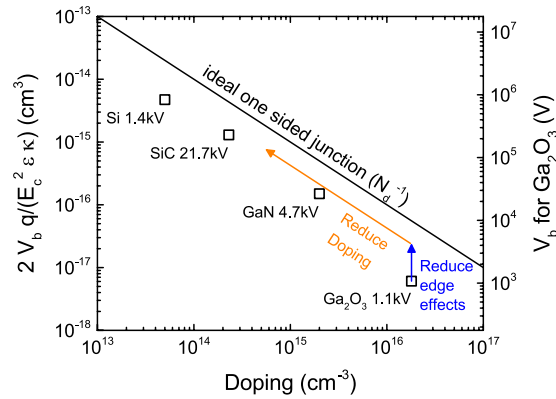
Figure 1. Normalized breakdown voltage (left axis) vs. doping concentration for single-sided junction power devices. The ideal relationship assuming the full-depletion approximation and 1D electrostatics is shown by the black line. The right axis indicates the projected absolute breakdown voltage for Ga_2O_3 devices for comparison. Square symbols indicate experimental measurements of devices with breakdown voltages among the highest reported for each material: Si[38], SiC[39], GaN[40], Ga_2O_3[7].

more mature materials, it is clear that some improvement can be expected from the optimization of device geometries to mitigate edge effects, as shown by the blue arrow. However, much greater improvement in breakdown voltage is possible from reducing drift layer doping in Ga_2O_3 devices, as indicated by the orange arrow. For instance, if the drift layer doping of a Ga_2O_3 device can be reduced to about 10^{14} cm^{-3} like the 21.7 kV SiC device indicated in Fig. 1, then the Ga_2O_3 device will have a breakdown voltage over 100 kV as indicated by the right axis of Fig. 1. Therefore, understanding and mitigating unintentional doping in Ga_2O_3 is key to increasing the maximum achievable breakdown voltages in Ga_2O_3 beyond the recently demonstrated 1 kV devices[7].

With these motivations, we have undertaken transport and capacitance spectroscopy studies in order to better understand the origin of unintentional doping in Ga_2O_3. The transport properties of commercially available unintentionally doped ($\bar{2}01$) Ga_2O_3 substrates from Tamura Corporation grown via the EFG method[13,14] are characterized via temperature dependent Hall effect measurements. High temperature Hall effect measurements up to 1000 K reveal a previously unobserved unintentional donor with an energy level 110 meV below the conduction band edge in addition to previously observed shallow donors attributed to Si[14,17]. To confirm the existence of this unintentional donor, temperature dependent admittance spectroscopy measurements were performed on a Ga_2O_3 Schottky diode structure, with an activation energy of 131 meV observed via this technique. This activation energy agrees well with the donor energy of 110 meV determined via Hall effect measurements. Finally, using the information obtained from the temperature dependent Hall effect measurements, the effects of the 110 meV donor on the specific on-resistance (R_{onsp}) of Ga_2O_3 Schottky diodes are assessed via analytical calculations, indicating that incomplete ionization of the 110 meV donor increases the R_{onsp} and reduces breakdown voltage as compared to Ga_2O_3 devices with only the shallow donor, beyond the usual tradeoff between on-resistance and breakdown voltage.

Results

Hall Effect Measurements.
Figure 2 shows the temperature dependent carrier density, normalized to room temperature, as measured by the Hall effect for two samples. The Hall scattering factor was assumed to be one when calculating the carrier density. The temperature dependent conductivity, mobility, and analysis of the relevant scattering mechanisms for these same samples can be found in the supplementary information. With the increased slope of the log-reciprocal plot from room temperature up to about 450 K, the temperature dependence of the carrier density must be determined by two donors with different energy levels. To estimate the donor energy levels, the data was fit with a model consisting of two donors with a compensating acceptor as shown in Equation (1):

$$N_c e^{\frac{E_f - E_c}{kT}} + N_a = \frac{N_{d1}}{1 + 2e^{\frac{E_f - E_{d1}}{kT}}} + \frac{N_{d2}}{1 + 2e^{\frac{E_f - E_{d2}}{kT}}}$$

(1)

where N_c is the effective density of states in the conduction band, N_{d1} and N_{d2} the concentrations of the two donors, N_a the concentration of compensating acceptors, E_c the energy of the conduction band edge, E_f the Fermi level, E_{d1} and E_{d2} the donor energies. An effective mass $m^* = 0.3m_0$[18–20] was used to estimate N_c analytically[21], while N_{d1}, N_{d2}, E_{d1}, E_{d2}, and N_a are free parameters. The values of the free parameters are summarized in Table 1, and the resulting fit is plotted as a black line in Fig. 2. The model indicates that the increased slope from 300 K to 450 K is the result of a higher energy donor with energy 110 meV. Additionally, a shallow donor is also observed with energy 23 meV, previously identified as silicon from glow discharge mass spectrometry (GDMS) analysis of Tamura samples[22]. Carrier activation in previous studies of Ga_2O_3 was well described by a single shallow donor which they also attributed to unintentional silicon dopants;[14,17] however, the second higher energy donor has not been observed previously.
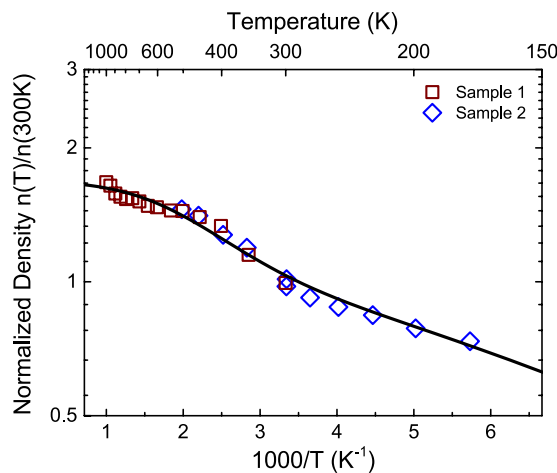
Figure 2. Hall carrier density (log scale) vs. 1000/T of Ga_2O_3 for two samples measured in the square geometry. The data are normalized to the Hall carrier density at 300 K. The symbols are the measured data and the black line a fit. Room temperature electron densities are 1.71×10^{17} cm^{-3} for Sample 1 (red square) and 1.21×10^{17} cm^{-3} for Sample 2 (blue diamond).

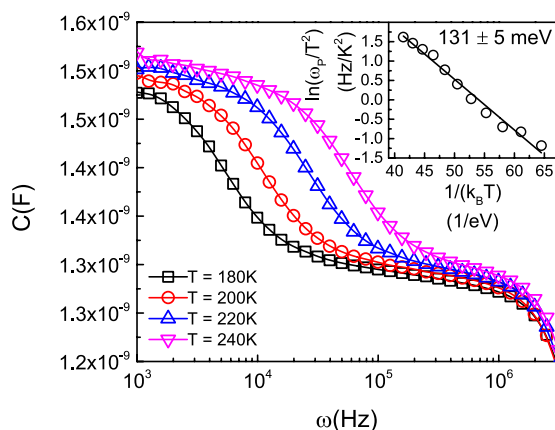**Figure 3.** Frequency dependent capacitance (C-f) data at different temperatures (T) indicating the unintentional donor. Inset: Arrhenius plot [ln(ω_p/T^2) vs 1/(k$_B$T)] for the trap signature observed through admittance spectroscopy in which ω_p is the negative peak in the $\omega dC/d\omega$ vs ω spectrum. The activation energy is extracted from the slope (fitted line). This activation energy matches that determined for the unintentional donor via Hall effect measurement.

N_{d1}	(cm^{-3})	7.5×10^{16}
$E_c - E_{d1}$	(meV)	110
N_{d2}	(cm^{-3})	1.4×10^{17}
$E_c - E_{d2}$	(meV)	23
N_a	(cm^{-3})	1.0×10^{16}

Table 1. Parameters for the carrier density vs. temperature model.

Admittance Spectroscopy Measurements. Admittance spectroscopy measurements confirm the existence of the previously unobserved donor. Figure 3 shows capacitance of a Ga_2O_3 Schottky diode as a function of frequency for several temperatures. The C vs. ω spectrum exhibits a step transition separating two plateaus, C_d at $\omega < \omega_p$ and C_g at $\omega > \omega_p$, which indicates the presence of a trap state. The transition frequency, ω_p, corresponds to the carrier emission rate from the trap level. To determine the activation energy of the trap state, ω_p was obtained from the negative peak in the differential capacitance ($\omega dC/d\omega$ vs ω) spectrum to construct an Arrhenius plot of ln(ω_p/T^2) vs 1/(k$_B$T), shown in Fig. 3 inset. From the slope of the plot, the activation energy of the trap is determined to be $E_a = 131 \pm 5$ meV[23]. Furthermore, the trap density, calculated from the height of the capacitance step[23], is $N_t = 4.4 \times 10^{16}$ cm^{-3}. A relative dielectric constant of 10 for Ga_2O_3 was used for this calculation[24,25]. These data

are well matched to the previously unobserved donor identified via Hall effect measurements, which indicated a donor energy of 110 meV and donor density of 7.5×10^{16} cm^{-3} as previously discussed. The small differences between the Hall effect measurements and admittance spectroscopy measurements are not surprising and are consistent with sample to sample variation within the two-inch Ga$_2$O$_3$ wafer from which the three samples were cut. Therefore, the trap state observed via admittance spectroscopy confirms the existence of the previously unobserved unintentional donor.

Possible Origins of the Donor. While the electrical characterization performed here cannot determine the chemical or crystallographic origin of the 110 meV donor, we nevertheless consider a few hypotheses. It is natural to ask if a native defect is responsible for the observed donor. DFT calculations rule out simple oxygen and gallium vacancies as they are determined to be deep donors[26] and acceptors[27,28], respectively. However, antisites and interstitials could be responsible. Extrinsic impurities, of course, could also be responsible for the donor, and glow discharge mass spectrometry (GDMS) analysis of Tamura substrates indicates the presence of several impurities whose dopant properties in Ga$_2$O$_3$ are unknown[22]. Last, silicon on the octahedrally coordinated Ga(II) site of Ga$_2$O$_3$ could be responsible for the 110 meV donor. DFT calculations indicate that Si prefers the tetrahedrally coordinated Ga(I) site in which it is a shallow donor;[26] however, STM analysis of Si donors near the (100) surface of Ga$_2$O$_3$ indicates that Si occupies both Ga(I) and Ga(II) lattice sites[29]. This fact suggests that Si on the Ga(II) site should also be considered as a possible origin of the 110 meV donor.

Discussion

These unintentional donors have implications for the performance of Ga$_2$O$_3$ based power devices; namely they reduce the maximum achievable breakdown voltage in a Ga$_2$O$_3$ power device. Because the doping of the drift-layer cannot be reduced below the level of unintentional doping, the density of unintentional donors sets the lower limit on electric field at the metal-semiconductor interface and the upper limit on the depletion width of the Ga$_2$O$_3$ drift-layer for a given applied voltage. Therefore, a limit is set on the tradeoff which allows higher breakdown voltage to be achieved at the expense of larger on-resistance. To mitigate the presence of previously identified silicon shallow donors in the substrate, several methods including LPCVD[30], MOCVD[31,32], HVPE[33,34], and MBE[2,3,35,36] have been used to grow homoepitaxial Ga$_2$O$_3$ layers on Ga$_2$O$_3$ substrates, achieving lower carrier densities by minimizing unintentional doping. However, the carrier concentration due to unintentional doping still remaining in epitaxial layers is typically 10^{15} to 10^{17} cm^{-3} [37]. This concentration is similar to the additional carrier concentration due to the 110 meV donor observed in these bulk samples considering incomplete ionization. For example, at a 110 meV donor concentration of 7.5×10^{16} cm^{-3} as found in this study, with no other donors or acceptors, 3.4×10^{16} cm^{-3} free electrons are thermally activated into the conduction band at 300 K for an ionization efficiency of 46%. These facts suggest that the 110 meV donor may also play a role in the unintentional doping of epitaxially grown Ga$_2$O$_3$, warranting further study but beyond the scope of this work. The importance of the high temperature Hall effect measurements and admittance spectroscopy measurements should be emphasized. As our calculation indicates, the higher activation energy of the 110 meV donors means that their ionization efficiency N_d^+/N_d is significantly less than 100% at room temperature. Therefore, room temperature and low temperature Hall measurement will not identify the full donor concentration, N_d, which determines the maximum breakdown voltage. Underestimating the concentration of donors could lead to an overestimate of the breakdown voltage without high temperature Hall effect measurements or admittance spectroscopy measurements like those performed in this study.

While unintentional shallow donors and the 110 meV donor both set a limit on the tradeoff between on-resistance and breakdown voltage, the 110 meV donor poses an additional challenge to maximizing breakdown voltage and minimizing on-resistance due to its four times larger donor energy as compared to the shallow donor. Because of the higher donor energy, incomplete ionization of the 110 meV donor is more severe than for the shallow donor, degrading the specific on-resistance vs. breakdown voltage characteristic for Ga$_2$O$_3$ based devices. The 110 meV donor is shallow enough in energy that it becomes fully ionized when the Schottky diode is reverse biased, reducing the depletion width, increasing the electric field at the metal-semiconductor interface, and reducing the breakdown voltage in the same way as the shallow donor. However, the 110 meV donor energy is large enough that incomplete ionization can be significant, meaning that only a fraction of the 110 meV donors are ionized when the Schottky diode is forward biased, reducing the carrier concentration available to conduct the on-current. To quantitatively examine those effects, specific on-resistance (R$_{onsp}$) versus breakdown voltage characteristics have been calculated for Ga$_2$O$_3$ Schottky diode devices including the incomplete ionization effect, with the results plotted in Fig. 4. Details of the calculation can be found in the supplementary information. As Fig. 4 shows, the on-resistance versus breakdown voltage characteristics are degraded where the maximum breakdown voltage decreases and the on-resistance increases as the concentration of the 110 meV donor increases. To determine the maximum acceptable concentration of 110 meV donors for a particular target breakdown voltage, the percent increase in R$_{onsp}$ is calculated for a Schottky diode containing both 110 meV donors and shallow donors versus a Schottky diode containing only shallow donors designed for the same breakdown voltage. The results of the calculation are plotted in Fig. 5 with additional details available in the supplementary information. With Fig. 5, we can estimate the maximum concentration of the 110 meV donors acceptable for 10 kV operation of Ga$_2$O$_3$ Schottky diode devices. To limit the increase in R$_{onsp}$ to one percent, the concentration of 110 meV donors must be less than 5×10^{14} cm^{-3}. A similar analysis of the percent decrease in breakdown voltage due to 110 meV donors is also presented in the supplementary information.

In conclusion, high temperature Hall effect and admittance spectroscopy measurements have revealed a previously unobserved unintentional donor with energy 110 meV below the conduction band edge in commercially available unintentionally doped Ga$_2$O$_3$ substrates grown by the EFG method. The existence of these unintentional donors sets a limit on the maximum breakdown voltages that can be achieved in Ga$_2$O$_3$ devices and must be mitigated to achieve the full benefits of Ga$_2$O$_3$ based power electronics. Additionally, incomplete ionization of the 110 meV donor causes increased on-resistance and decreased breakdown voltage in diodes containing the donor,
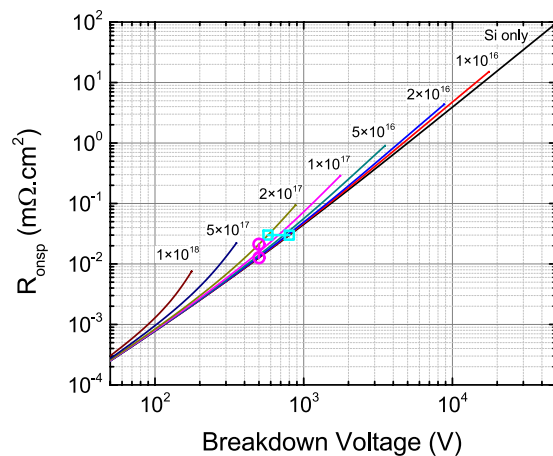
Figure 4. Analytical calculation of specific on-resistance (R_{onsp}) vs. breakdown voltage for Ga_2O_3 based Schottky junction devices with 110 meV donors including the effects of incomplete ionization. The label for each curve indicates the fixed concentration of 110 meV donors in units of cm^{-3}. The pink circles, cyan squares, and line segments illustrate the relationship to Fig. 5 and Figure S3 as described in the supplementary information.
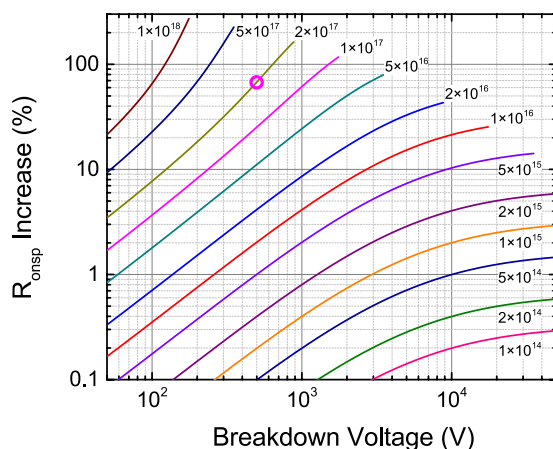

Figure 5. Percent increase in specific on-resistance (R_{onsp}) due to incomplete ionization as a function of breakdown voltage comparing Ga_2O_3 Schottky diodes with 110 meV donors to those without. The labels indicate the fixed concentration of 110 meV donors in cm^{-3} for each curve. The pink circle illustrates the relationship to Fig. 4 as described in the supplementary information.

as compared to diodes containing only the shallow donor, beyond the usual tradeoff between on-resistance and breakdown voltage. To achieve 10 kV operation in Ga_2O_3 Schottky diode devices, analysis indicates that the concentration of 110 meV donors much be reduced below $5 \times 10^{14} cm^{-3}$ to limit the increase in R_{onsp} to one percent.

Methods

Sample Fabrication and Measurement. Two van der Pauw test samples were diced from the same two inch wafer into 1 cm × 1 cm square pieces. Following dicing, samples were solvent cleaned and 50 nm/1000 nm Ti/Au contacts were sputtered on the sample corners. To improve contact resistance, the samples were annealed from room temperature up to 450 °C with a 15 min ramp in a tube furnace with argon gas flow. A third sample from the same two inch wafer was prepared for admittance spectroscopy by depositing an indium tin oxide (ITO) transparent contact to form a Ga_2O_3 Schottky diode. Following device fabrication, temperature dependent van der Pauw and Hall effect measurements were carried out in two separate Hall effect measurement systems. An electromagnet with vacuum cryostat and closed-loop He refrigerator was used for measurements below room temperature, while an electromagnet with a quartz tube furnace with silicon carbide heater was used for measurements above room temperature. The samples were kept under nitrogen gas flow at atmospheric pressure during high temperature measurements. Admittance spectroscopy measurements were carried out under vacuum in a closed-loop He cryostat using a Keysight Agilent 4990 A impedance analyzer.

Data Availability. The data that support the findings of this study are available on request from the corresponding author S.M.

References

1. Koshi, K. *et al*. β-Ga$_2$O$_3$-Based Single Crystal Substrate. *U.S. Patent 9* **349**, 915 (2016).
2. Higashiwaki, M., Sasaki, K., Kuramata, A., Masui, T. & Yamakoshi, S. Gallium oxide (Ga$_2$O$_3$) metal-semiconductor field-effect transistors on single-crystal β-Ga$_2$O$_3$ (010) substrates. *App. Phys. Lett.* **100**, 013504 (2012).
3. Higashiwaki, M. *et al*. Depletion-mode Ga$_2$O$_3$ metal-oxide-semiconductor field-effect transistors on β-Ga$_2$O$_3$ (010) substrates and temperature dependence of their device characteristics. *App. Phys. Lett.* **103**, 123511 (2013).
4. Green, A. J. *et al*. 3.8-MV/cm breakdown strength of MOVPE-grown Sn-doped β-Ga$_2$O$_3$ MOSFETs. *IEEE Electron Device Lett* **37**, 902–905 (2016).
5. Wong, M. H., Sasaki, K., Kuramata, A., Yamakoshi, S. & Higashiwaki, M. Field-plated Ga$_2$O$_3$ MOSFETs with a breakdown voltage of over 750 V. *IEEE Electron Device Lett* **37**, 212–215 (2016).
6. Chabak, K. D. *et al*. Enhancement-mode Ga$_2$O$_3$ wrap-gate fin field-effect transistors on native (100) β-Ga$_2$O$_3$ substrate with high breakdown voltage. *App. Phys. Lett.* **109**, 213501 (2016).
7. Konishi, K. *et al*. 1-kV vertical Ga$_2$O$_3$ field-plated Schottky barrier diodes. *App. Phys. Lett.* **110**, 103506 (2017).
8. Ueda, N., Hosono, H., Waseda, R. & Kawazoe, H. Synthesis and control of conductivity of ultraviolet transmitting β-Ga$_2$O$_3$ single crystals. *App. Phys. Lett.* **70**, 3561–3563 (1997).
9. Tomm, Y., Ko, J. M., Yoshikawa, A. & Fukuda, T. Floating zone growth of β-Ga$_2$O$_3$: a new window material for optoelectronic device applications. *Sol. Energy Mater. Sol. Cells* **66**, 369–374 (2001).
10. Víllora, E. G., Shimamura, K., Yoshikawa, Y., Aoki, K. & Ichinose, N. Large-size β-Ga$_2$O$_3$ single crystals and wafers. *J. Cryst. Growth* **270**, 420–426 (2004).
11. Suzuki, N. *et al*. Fabrication and characterization of transparent conductive Sn-doped β-Ga$_2$O$_3$ single crystal. *Phys. Status Solidi (c)* **4**, 2310–2313 (2007).
12. Víllora, E. G., Shimamura, K., Yoshikawa, Y., Ujiie, T. & Aoki, K. Electrical conductivity and carrier concentration control in β-Ga$_2$O$_3$ by Si doping. *App. Phys. Lett.* **92**, 202120 (2008).
13. Aida, H. *et al*. Growth of β-Ga$_2$O$_3$ single crystals by the edge-defined, film fed growth method. *Jpn. J. Appl. Phys.* **47**, 8506 (2008).
14. Oishi, T., Koga, Y., Harada, K. & Kasu, M. High-mobility β-Ga$_2$O$_3$ single crystals grown by edge-defined film-fed growth method and their Schottky barrier diodes with Ni contact. *Appl. Phys. Expr* **8**, 031101 (2015).
15. Tomm, Y., Reiche, P., Klimm, D. & Fukuda, T. Czochralski grown β-Ga$_2$O$_3$ crystals. *J. Cryst. Growth* **220**, 510–514 (2000).
16. Galazka, Z. *et al*. Czochralski growth and characterization of β-Ga$_2$O$_3$ single crystals. *Cryst. Res. Technol.* **45**, 1229–1236 (2010).
17. Irmscher, K., Galazka, Z., Pietsch, M., Uecker, R. & Fornari, R. Electrical properties of β-Ga$_2$O$_3$ single crystals grown by the Czochralski method. *J. Appl. Phys.* **110**, 063720 (2011).
18. He, H. *et al*. First-principles study of the structural, electronic, and optical properties of Ga$_2$O$_3$ in its monoclinic and hexagonal phases. *Phys. Rev. B* **74**, 195123 (2006).
19. Peelaers, H. & Van, C. G. Brillouin zone and band structure of β-Ga$_2$O$_3$. *Phys. Status Solidi (b)* **252**, 828–832 (2015).
20. Furthmüller, J. & Bechstedt, F. Quasiparticle bands and spectra of Ga$_2$O$_3$ polymorphs. *Phys. Rev. B* **93**, 115204 (2016).
21. Sze, S. M. and Kwok, K. N., *Physics of Semiconductor Devices, 3rd ed.* John Wiley & Sons, 17–18 (2007).
22. Kuramata, A. *et al*. High-quality β-Ga$_2$O$_3$ single crystals grown by edge-defined film-fed growth. *Jpn. J. Appl. Phys.* **55**, 1202A2 (2016).
23. Blood, P. and Orton, J.W., *The Electrical Characterization of Semiconductors: Majority Carries and Electron States*. Academic Press (1992).
24. Hoeneisen, B., Mead, C. A. & Nicolet, M. A. Permittivity of β-Ga$_2$O$_3$ at low frequencies. *Solid-State Electron* **14**, 1057–1059 (1971).
25. Schubert, M. *et al*. Anisotropy, phonon modes, and free charge carrier parameters in monoclinic β-gallium oxide single crystals. *Phys. Rev. B* **93**, 125209 (2016).
26. Varley, J. B., Weber, J. R., Janotti, A. & Van, C. G. Oxygen vacancies and donor impurities in β-Ga$_2$O$_3$. *App. Phys. Lett.* **97**, 142106 (2010).
27. Korhonen, E. *et al*. Electrical compensation by Ga vacancies in Ga$_2$O$_3$ thin films. *App. Phys. Lett.* **106**, 242103 (2015).
28. Varley, J. B., Peelaers, H., Janotti, A. & Van, C. G. Hydrogenated cation vacancies in semiconducting oxides. *J. Phys.: Condens. Matter* **23**, 334212 (2011).
29. Iwaya, K., Shimizu, R., Aida, H., Hashizume, T. & Hitosugi, T. Atomically resolved silicon donor states of β-Ga$_2$O$_3$. *App. Phys. Lett.* **98**, 142116 (2011).
30. Rafique, S. *et al*. Homoepitaxial growth of β-Ga$_2$O$_3$ thin films by low pressure chemical vapor deposition. *App. Phys. Lett.* **108**, 182105 (2016).
31. Wagner, G. *et al*. Homoepitaxial growth of β-Ga$_2$O$_3$ layers by metal-organic vapor phase epitaxy. *Phys. Status Solidi (a)* **211**, 27–33 (2014).
32. Du, X. *et al*. Characterization of homoepitaxial β-Ga$_2$O$_3$ films prepared by metal-organic chemical vapor deposition. *J. Cryst. Growth* **404**, 75–79 (2014).
33. Murakami, H. *et al*. Homoepitaxial growth of β-Ga$_2$O$_3$ layers by halide vapor phase epitaxy. *Appl. Phys. Expr* **8**, 015503 (2014).
34. Higashiwaki, M. *et al*., Ga$_2$O$_3$ Schottky barrier diodes with n$^-$ Ga$_2$O$_3$ drift layers grown by HVPE. *73rd Annual Device Research Conference (DRC)*, 29–30 (2015).
35. Víllora, E.G., Shimamura, K., Kitamura, K., and Aoki, K., RF-plasma-assisted molecular-beam epitaxy of β-Ga$_2$O$_3$. *App. Phys. Lett*. **88** (2006).
36. Sasaki, K. *et al*. Device-quality β-Ga$_2$O$_3$ epitaxial films fabricated by ozone molecular beam epitaxy. *Appl. Phys. Expr* **5**, 035502 (2012).
37. Higashiwaki, M. *et al*. Recent progress in Ga$_2$O$_3$ power devices. *Semicond. Sci. Technol.* **31**, 034001 (2016).
38. Yilmaz, H. Optimization and surface charge sensitivity of high-voltage blocking structures with shallow junctions. *IEEE Trans. Electron Devices* **38**, 1666–1675 (1991).
39. Niwa, H., Feng, G., Suda, J., and Kimoto, T., Breakdown characteristics of 12–20 kV-class 4H-SiC PiN diodes with improved junction termination structures. *24th International Symposium on Power Semiconductor Devices and ICs*, 381–384 (2012).
40. Ohta, H. *et al*. Vertical GaN p-n junction diodes with high breakdown voltages over 4 kV. *IEEE Electron Device Lett* **36**, 1180–1182 (2015).

Acknowledgements

Author Contributions

S.M. initiated the project. A.T.N. and S.M. performed and analyzed Hall effect measurements. R.L. and J.V.L. performed and analyzed admittance spectroscopy measurements. A.T.N. and S.M. wrote the manuscript with input from J.V.L., D.B.T., K.D.C., and G.H.J. S.M. supervised the project.

Additional Information

Supplementary information accompanies this paper at https://doi.org/10.1038/s41598-017-13656-x.

Competing Interests: The authors declare that they have no competing interests.

Publisher's note: Springer Nature remains neutral with regard to jurisdictional claims in published maps and institutional affiliations.